JOURNAL OF MATERIALS SCIENCE 26 (1991) 4997–5003

Mechanical characterization by dynamical tensile loading of 2017 aluminium alloy joints welded by diffusion bonding

M. CAILLER*‡, O. DEBBOUZ*, M. DANNAWI§, T. LATOUCHE*
*Laboratoire de Sciences des Surfaces et Interfaces, ISITEM, Université de Nantes, La Chantrerie, CP 3023, 44087 Nantes Cédex 03, France
§Laboratoire des Structures, ENSM, 1 rue de la Noë, 44072 Nantes Cédex, France

The mechanical properties of diffusion-welded joints of 2017 aluminium–copper alloys have been studied under dynamic loading with the help of a Hopkinson bar linear assembly. With the aim of comparing with previous results obtained under static loading, the strength, failure elongation and failure energy were evaluated in the welding temperature range from 475 to 600 °C. Measurements of the above mechanical properties were also performed on treated specimens which were base-material specimens subjected to the same thermal cycle as the welded samples. It was found that for a welding temperature above 525 °C the strength of the welded joints could reach values of the same order of magnitude as those of the treated samples. In contrast, the failure elongation and failure energy remained clearly lower, whatever the welding temperature was. For a given value of the welding pressure, the welding temperature dependence rate of the dynamic strength was shown to be increased with increasing welding time. With regard to the failure elongation or the relatively weak influence of the welding pressure on the joint strength, the spread in the experimental results (probably arising from the brittle nature of the sample failure mode) does not allow a clear conclusion. In spite of this restriction, it can be concluded that differences in the mechanical properties of the diffusion-welded joints could be evidenced by dynamic loading tests, even if no significant differences could be observed under static loading.

1. Introduction

Diffusion welding is a solid-state joining technique which, by avoiding problems due to fusion, is *a priori* well adapted for welding materials exhibiting a high solidification crack susceptibility [1, 2]. The age-hardenable aluminium–copper alloy 2017, which is increasingly employed in the aerospace industry, is a good example of this type of material. Diffusion welding allows also the realization of pieces net to dimensions, making the process less material-consuming than machining.

However, the non-destructive industrial testing of diffusion-bonded joints is still difficult, so that it is necessary to determine very precisely in the laboratory the working conditions required to obtain the highest values of the welded bond mechanical properties. This is a very long task because of the great number of process parameters.

The influence of the main welding parameters (time, temperature, pressure, atmosphere and surface preparation) on the mechanical properties of A2017 alloy welded joints has been previously studied under static loading [3–7]. In such studies, it was found that, for temperatures lower than 525 °C and for reasonably short welding times, the strength of the joints was small in comparison with that of the base material [5–7]. In contrast, above 525 °C strengths close to that of the bulk material could be reached, though the elongation at failure of the welded samples remained very weak and rupture occurred near the initial interface.

Observations by scanning electron microscopy (SEM) have shown that at lower welding temperatures the failure surfaces presented a brittle fracture aspect, whereas for welding temperatures higher than 525 °C the failure surface exhibited many dimples characteristic of a ductile fracture. It was therefore expected that the differences in the welded sample strength values according to the brittle (at lower welding temperatures) or ductile (at higher welding temperatures) nature of the failure should be made more obvious by increasing the loading rate. This is the reason why, with the aim of completing the mechanical characterization of the A2017 diffusion-welded joints, we have undertaken a series of dynamic tests with the help of a Hopkinson bar assembly line.

2. Base material and welding process

The base material was the commercial aluminium–copper alloy A2017 (supplied in T4 metallurgical

‡To whom correspondence should be addressed.

0022–2461/91 $03.00 + .12

TABLE I Chemical composition of the base material (wt %)

	Si	Fe	Cu	Mn	Mg	Cr	Zn	Ti + Zr	Al
Min.	0.2		3.5	0.4	0.4				Balance
Max.	0.8	0.7	4.5	1.0	1.0	0.1	0.25	0.25	Balance

state), the chemical composition of which is given in Table I.

After machining of the two pieces to be welded, the faying surfaces were manually polished with emery paper (grades 600 and 1200). Then, the pieces were cleaned in an ultrasonic bath of acetone and finally dried in a hot air flow. Immediately after this surface preparation, the pieces were placed in the welding apparatus so that the polished grooves of the two faying surfaces were in crossed positions.

The diffusion welding was carried out at a pressure of about 10^{-4} Pa using the experimental set-up described previously [5]. External pressure was applied on the pieces only when the welding temperature was reached, and it was maintained at a constant value throughout the welding process and during the major part of the cooling step.

3. Mechanical characterization of welded joints by dynamic loading

3.1. Sample preparation

With the aim of comparison, all the samples tested in dynamic loading were welded by using the same general procedure as that used for samples statically tested. The welding temperature was changed from 475 to 600°C and for each temperature three samples were welded, two with a welding pressure of 2 MPa and one with 5 MPa. In the former case, the welding time was fixed at either 30 min or 2 h whereas in the latter case the welding time was 30 min. These ranges of values are quite similar to those used for the statically loaded samples. Hence it is expected that, by completing the results of our previous studies, the new information so obtained could help us to find the best choice of welding parameters.

After welding the samples were machined in order to present in their central part a cylindrical shape of 5 mm diameter and 30 mm length (Fig. 1). The two extremities of the specimen were threaded so as to fix it on the two Hopkinson bars of the test apparatus described below.

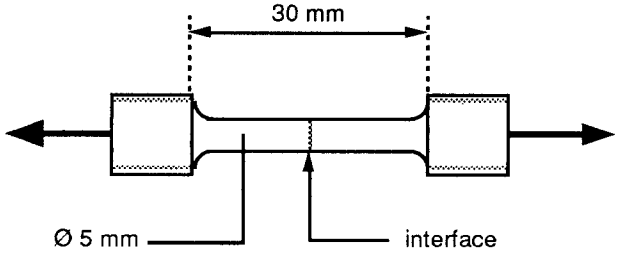

Figure 1 Shape of the dynamical tensile-tested samples.

3.2. Dynamic loading test

The dynamic tensile loading tests were carried out on a dynamic linear assembly with two Hopkinson bars (Fig. 2). One of these bars is 2 m long and is called the entrance bar. The second bar is 1 m long and is called the exit bar. The sample is disposed between the two bars in which it is fixed by screwing at its two extremities. The technique involves the creation of an elastic compression wave into the entrance bar under the impact of a projectile moving at a given velocity v. In order to proceed to a dynamic tensile loading test, this compression wave then has to be changed into a tensile stress in the sample. For this purpose the compression wave created in the entrance bar is transmitted to the exit bar through a drilled ring 32 mm long which is disposed between the two bars and around the sample. The inner and outer diameters of the ring (D_{inn} = 11 mm, D_{out} = 19.4 mm) were chosen in order to allow a transmission as total as possible of the compression wave through the ring. However, some perturbations can be generated because of the impedance discontinuities at the interface between the ring and the bars. The reflected waves arising from these perturbations move into the entrance bar to the left-hand end, where they are reflected before moving back to the ring. The entrance bar was made sufficiently long to suppress interference between these perturbation effects and the measurement signal of the sample.

The assembly comprising the two bars, the ring and the sample, slides freely as a whole on fixed supports. The compression wave transmitted from the entrance to the exit bar then moves to the free right-hand end of the line where it is reflected back. By reflection at the free end of the line, the compressive incident wave is transformed into a tensile wave which propagates to the sample. The ring, which assured a close contact between the two bars in the case of the compressive incident wave, no longer assures the same effect for the tensile reflected stress wave. The latter is therefore applied to the sample to be tested. In fact, it is partly transmitted to the entrance bar through the sample (up to the failure of this sample) and partly reflected at the interface between the sample and the exit bar. In order to collect these two signals without interference and without disturbance by the perturbation reflected waves described above, two stress-gauge bridges were judiciously placed on the entrance and the exit bar, respectively at 100 and 500 mm from the sample (see Fig. 2).

The load exerted on the sample was evaluated by measuring the tensile stress wave $\sigma_1(t)$ transmitted by the sample to the entrance bar, with the help of the stress-gauge bridge disposed on this entrance bar. Similarly, the wave $\sigma_2(t)$ reflected at the left-hand end of the exit bar was measured with the help of the

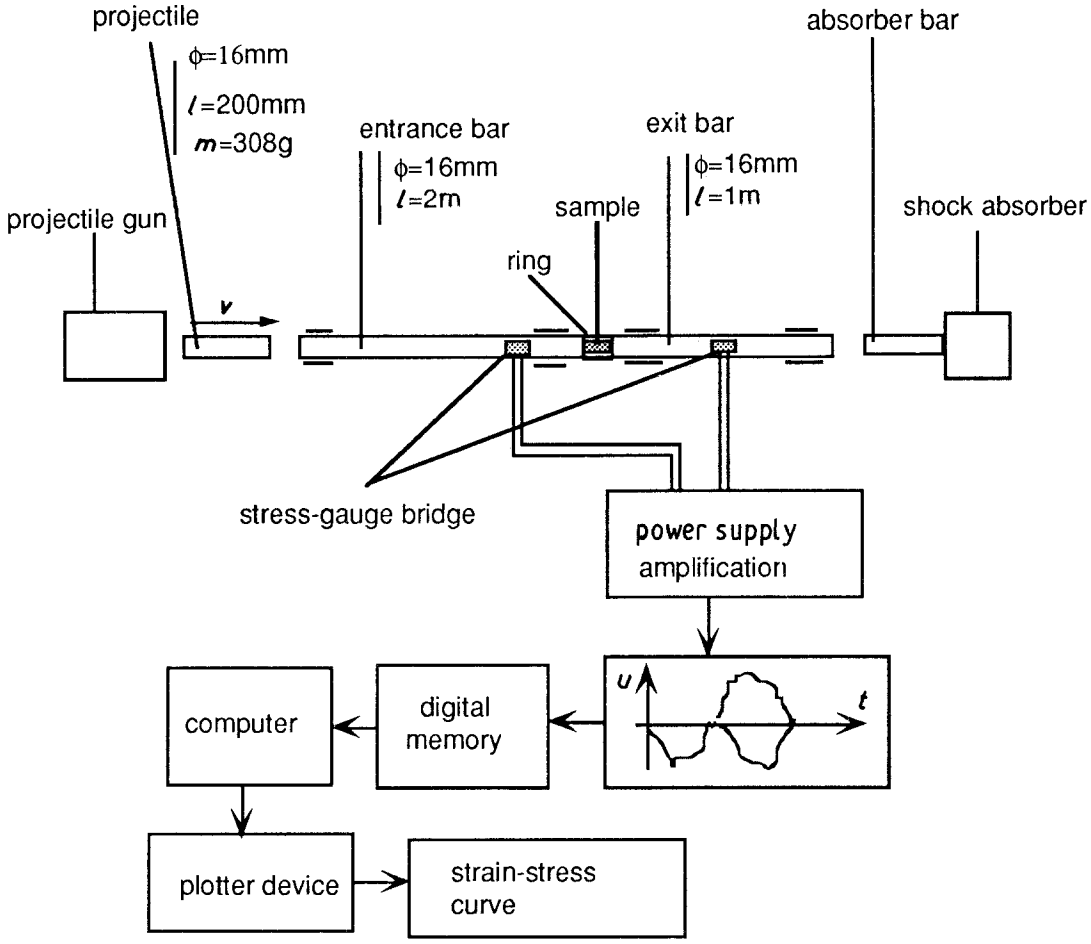

Figure 2 Dynamic Hopkinson bar assembly as adapted for traction-loading testing of the samples.

strain-gauge bridge disposed on the exit bar. The signals obtained were recorded on a memory oscilloscope and computerized. After failure of the sample, the assembly was projected on to a shock-absorber device and the measurements were stopped.

From a knowledge of the reflected and the transmitted stress waves, it is possible to calculate the stress exerted at time t on the sample from

$$\sigma(t) = \frac{\sigma_1(t)S[1 - \varepsilon(t)]}{S_0}$$

and the strain from

$$\varepsilon(t) = \frac{c}{EL_0}\int_0^t [\sigma_2(t) - \sigma_1(t)]\,dt$$

where c is the wave velocity in the Hopkinson bars, E and S the Young's modulus and the cross-section of these bars, respectively ($E = 1.89 \times 10^{11}$ Pa), L_0 the initial length of the sample and S_0 its initial cross-section.

Fig. 3 exhibits a diagram of the incident and reflected waves and superposed on it, the diagram of the

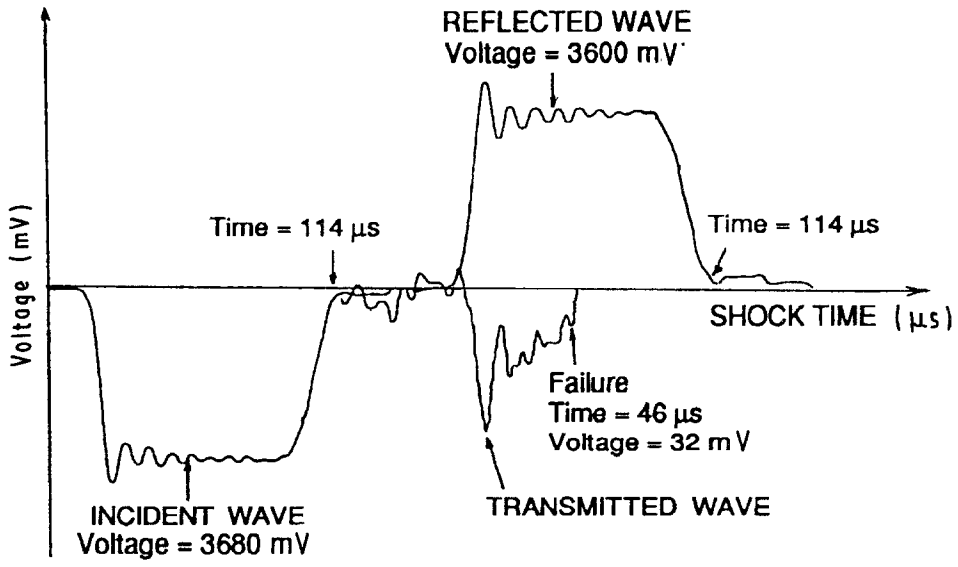

Figure 3 Diagram showing the incident, reflected and tensile stress waves.

wave transmitted through the sample which generates the dynamic loading of this sample. As can be seen, from a comparison of the reflected and transmitted signals, the time duration of the transmitted wave is substantially shorter than that of the reflected wave. This is evidence of the failure of the sample under the tensile stress wave effect.

4. Experimental results and discussion

4.1. Dynamic stress–elongation behaviour law

Dynamic tensile tests were carried out on different commercial rods of A2017 supplied in the T4 state. The results obtained on this type of sample showed that the tensile strengths reached values between 460 and 500 MPa, with total elongations ranging from 15 to 18%. These results cannot however be used as a reference for a direct comparison with the welded sample strengths. Indeed, the mechanical properties of the two welded pieces are more or less strongly modified by the thermal treatment imposed during the welding procedure. Therefore, for a more realistic comparison, it is necessary to measure the dynamic mechanical properties of the base material after this thermal cycle. For this, base material samples were heated to the welding temperature, maintained at this temperature for 30 min and then cooled under the same conditions as the welded samples. In what follows, such samples will be called the thermally treated samples or shortly, the treated samples.

The dynamic mechanical properties of the samples thermally treated at 550 °C for 30 min are exhibited in Fig. 4 (curve 1), where they are compared with those of a sample welded for 30 min at 550 °C under a welding pressure of 2 MPa (curve 2). As can be seen from Fig. 4, the dynamic behaviour of the two samples is almost identical at lower values of the elongation. The main difference arises from the fact that the welded sample fails for an elongation of less than 2%, whereas the failure elongation of the treated sample is at least 13%, i.e. 6 to 7 times that of the welded sample. Consequently, the strength of the welded sample is limited to 230 MPa whereas that of the treated sample reaches 300 MPa. Such a difference was also observed in static loading tests, but in that case the difference in the failure elongation values was found to be less important than under dynamic loading. Indeed, in static loading the failure elongation of the treated sample is about 22%, i.e. nearly three times that of the welded sample which is 7%. Still in static loading, the strength of the treated sample is about 380 MPa against 290 MPa for the welded sample. Therefore, the ratio between the strengths of the treated and the welded samples is nearly the same for dynamic loading and for static loading, at about 1.3.

It is worth noting that the stress–elongation curves present a large number of fluctuations which were interpreted as artifacts arising from reflections of the stress wave from the threaded parts of the sample. In spite of this difficulty, it was considered that it should be very interesting to evaluate the energy needed to break the samples by integrating the area under the curves, up to the failure elongation. From the results shown in Fig. 4, it was found that the rupture energy of the treated sample was larger than 32 J, whereas that of the welded sample was only about 2.6 J. The large difference between these two values comes essentially from the differences observed in the failure elongation values.

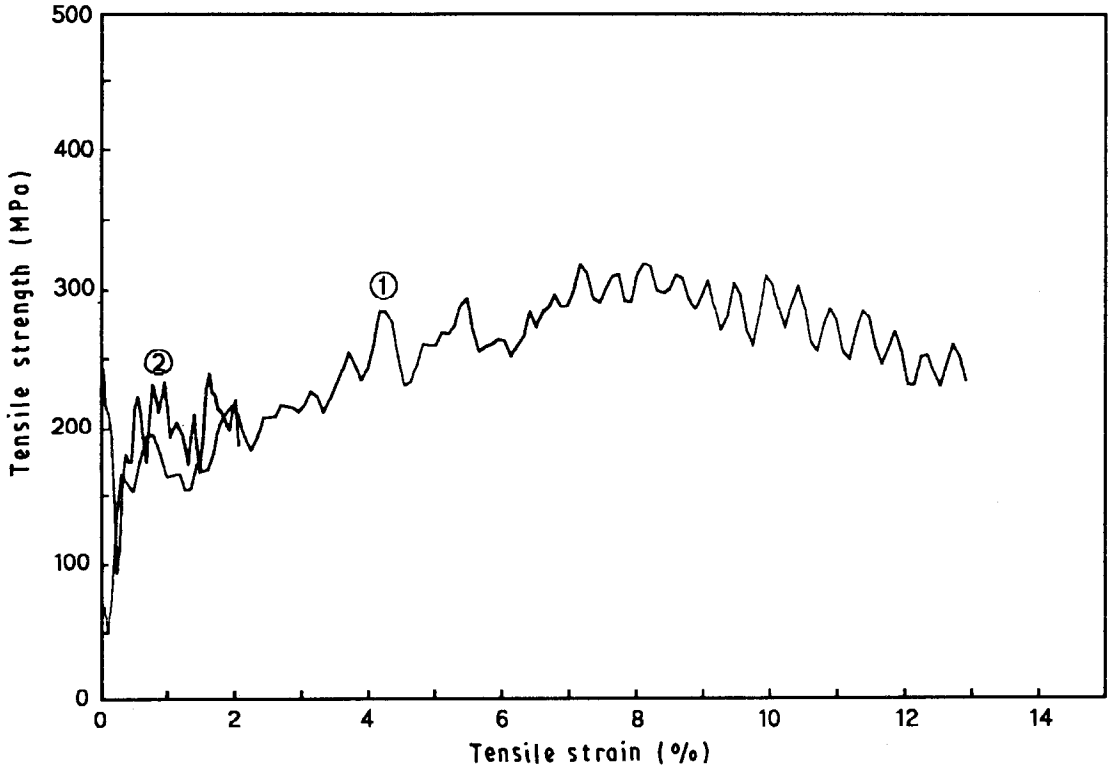

Figure 4 Dynamic stress–elongation behaviour laws for treated samples heated for 30 min at 550 °C (curve 1) and for samples welded for 30 min at 550 °C and 2 MPa (curve 2).

4.2. Influence of some process parameters

The strength, failure elongation and failure energy of the welded samples were investigated as a function of the welding temperature, for the three sets of welding pressure and welding time described in Section 3.1. With the aim of comparison, the above mechanical properties were also measured on treated samples heated to the welding temperature for 30 min.

In the temperature range studied, the strength of the treated samples is nearly constant within the experimental uncertainty, at about 340 MPa (Fig. 5). The strength of the welded joints itself remains at a substantially lower level as long as the temperature is below 525 °C. Above this temperature, the difference becomes much smaller and, within the experimental uncertainty, it can be considered that the strength of the welded sample is the same as that of the treated sample. This is in general agreement with the results obtained in static loading tests.

For a welding pressure of 2 MPa the rate of increase of the dynamic strength as a function of the welding temperature is clearly higher for a welding time of 2 h than for 30 min. Furthermore, it can be noticed that an increase in the values of the strength is still visible above 525 °C. The observations were somewhat more complex under static loading, to the extent that for a welding temperature under 525 °C, an increase in the welding time increased the strength of the welded samples, whereas above 525 °C no such increase was observed. For a fixed welding time of 30 min, the dynamic strength of the welded bonds is practically unchanged by an increase in the welding pressure from 2 to 5 MPa.

Fig. 6 exhibits similar results for the failure elongation. It is observed that for the treated samples, the failure strain is practically independent of the heating temperature, at about 13% (see also Fig. 4). Here, in contrast to the strength, the values obtained for the welded samples remain clearly smaller than those of the treated sample, at about 2 to 4%, whatever the welding temperature is. The effects of the other welding parameters appear to be small and without real significance. One can just observe that an increase in the welding time could slightly increase the failure strain. It is worth noting that the spread in the measurements is large, and may be related to the nature (probably brittle) of the failure. Therefore, to reduce the experimental uncertainty it would be necessary to carry out a large number of tests for each set of welding parameters and to deduce from the results a mean value for each measured mechanical property.

Similar considerations apply to the failure energy values of the welded joints (Fig. 7) and also probably to the failure energy of the treated sample at 600 °C, which is clearly higher than it is at lower temperatures. In spite of these limitations, the results of Fig. 7 show clearly that the failure energy of the welded joints is substantially lower than that of the treated samples. It can also be noticed that the spread in the measurements is reduced by increasing the welding time from 30 min to 2 h. In the latter case, it can then be observed that the failure energy follows a linear relationship with the welding temperature. On the other hand, for a welding time of 30 min the experimental uncertainty does not allow a clear observation of the welding temperature effects. However, it seems that, for a welding pressure of 2 MPa the failure energy remains very small as long as the welding temperature does not exceed 550 °C, but that at 575 °C it reaches a value of the same magnitude of that of the samples welded for 2 h.

4.3. Discussion

From the above results it is clear that the welding temperature must exceed 525 °C so that the joint

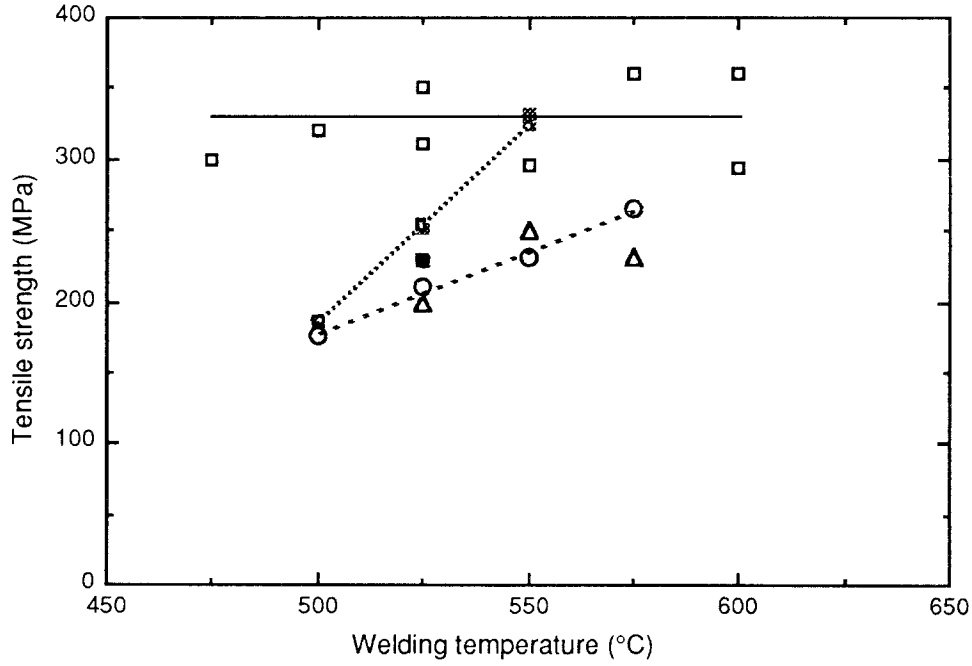

Figure 5 Results obtained for the strength as a function of the welding temperature for three different sets of the operating parameter values and for base material submitted to the same thermal cycle. (□) Base metal. Welded joints: (△) $P = 5$ MPa, $t = 30$ min; (○) $P = 2$ MPa, $t = 30$ min; (■) $P = 2$ MPa, $t = 2$ h.

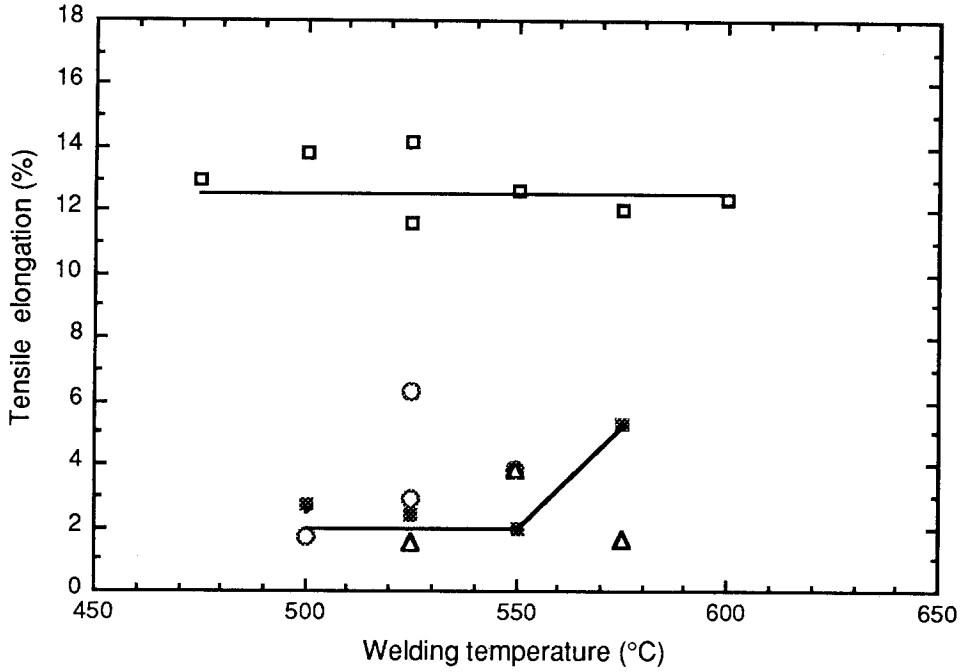

Figure 6 Results obtained for the failure strain as a function of the welding temperature for three different sets of the operating parameter values and for base material submitted to the same thermal cycle. (□) Base metal. Welded joints: (△) $P = 5$ MPa, $t = 30$ min; (○) $P = 2$ MPa, $t = 2$ h; (■) $P = 2$ MPa, $t = 30$ min.

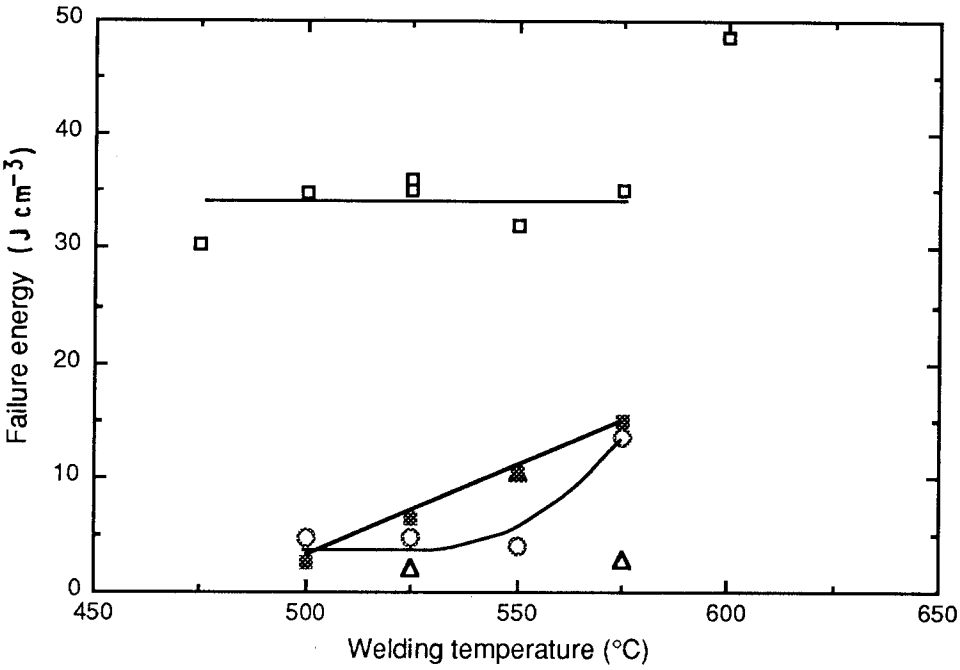

Figure 7 Results obtained for the failure energy as a function of the welding temperature for three different sets of the operating parameter values and for base material submitted to the same thermal cycle. (□) Base metal. Welded joints: (△) $P = 5$ MPa, $t = 30$ min; (○) $P = 2$ MPa, $t = 30$ min; (■) $P = 2$ MPa, $t = 2$ h.

strength reaches values close to that of the treated material. Similar observations were made in previous studies on the static loading strength [5] and it was also established that this temperature boundary is in fact the solidus temperature of the A2017 alloy. In other words, the presence of a liquid phase is needed to produce joints of high dynamic as well as high static strength.

From consideration of the failure strain or the failure energy it appears that the behaviour of the welded joints is substantially weakened compared to that of the base material, even if (as mentioned above) the strengths are in the same range of magnitude. Similar results were obtained under static loading, but in such a case it was observed that the differences between the measurements made on the welded joints and the treated samples were clearly less important. It was also observed that in every case the failure occurred in the interfacial region, even if the welded joint strength was as large as that of the treated material. This showed that the weaker part of the welded sample was always the joint region, probably because of its embrittlement. The differences between the behaviour of the welded and the treated samples are increased by

dynamic loading, so that it can be considered that embrittlement of the interface region is made more evident by loading the samples at high strain rates.

For a welding time of 30 min, an increase in the welding pressure from 2 to 5 MPa does not significantly improve the dynamic tensile joint strength. Now, such an increase in the welding pressure was previously shown as leading to an important increase in the welding deformation [5–7]. It can therefore be considered that any increase in the welding pressure, at least above 2 MPa, has to be avoided.

According to the present results, it seems that better welding conditions were obtained for a welding temperature above 525 °C, a welding time of 2 h and a welding pressure of 2 MPa. However, although in such a case the welded joint tensile strength is approximately equal to that of the base metal, the failure elongation and failure energy remain substantially lower than those of the treated sample. It is clear therefore that much additional work has to be done before reaching the optimum conditions for diffusion welding of A2017.

In order to better understand the phenomena arising during the welding operation, it should be interesting to proceed to an observation by scanning electron microscopy of the rupture surfaces, as was made for static loading tests. Also, energy-dispersive X-ray analyses of the interfacial region should bring complementary information on the metallurgic modifications produced. Such studies were carried out in the case of statically tested samples but not yet for the dynamic tested samples.

5. Conclusions

To the best knowledge of the authors the present work is the first study of the mechanical properties of diffusion-welded joints under high-rate tensile loading. The work was carried out on a Hopkinson bar linear assembly which was adapted in order to change the compressive wave generated by a projectile into a tensile wave applied to the sample. It has been shown that such a characterization brought definite information on the joint efficiency, and allowed one to display differences in the mechanical properties of the welded samples even if such differences were not visible under static loading. Some effects of the main operating parameters have been studied, the general trends of which have been evidenced. However, the spread in the measurements was found to be rather large, probably in relation to the brittle nature of the sample failure, so that detailed interpretations of some of the results have to be made with care. In spite of this restriction it is quite clear that an increase in the welding temperature enhances the strength of the joints. Above 525 °C, the joint strength reaches values of the same order of magnitude as those of base material samples submitted to the same thermal cycle (the treated samples). In contrast, the failure elongation of the welded joints remains very small and clearly lower than that of the treated samples, whatever the welding temperature is. The influence of the other welding parameters on the failure strain is not so well established. The failure energy of the welded joints increases with increasing welding temperature, but the effect is moderate because of the combination of the above-mentioned effects on the strength and the failure elongation. It can be noticed that the solidus temperature of A2017 is close to 525 °C, and that above this temperature a small amount of liquid phase coexists with the solid phase on the sample surface, which facilitates the bonding of the pieces to be welded.

In static tests, it appeared that above 525 °C the tensile strength of the diffusion-welded joints was practically independent of the other welding parameters (time, pressure, surface state). On the other hand, it was shown that in the same temperature range and for a welding pressure of 2 MPa, an increase in the welding time from 30 min to 2 h increased the tensile strength of the welded joints. Hence, it is concluded that high-rate tensile tests can be a very discriminating technique offering good prospects for determining the efficiency of diffusion-welded joints, and for helping in the choice of the best operating conditions.

References

1. B. BLANCHET, J. J. BOULANGER, F. BOULANGER and Y. LE PENVEN, *Soudage et Techniques Connexes* no. 3–4 (1975) 93.
2. M. SCHWARTZ, in Proceedings of Conference on Welding Technology for the Aerospace Industry, Las Vegas, October 1980 (1981) pp. 1–40.
3. T. ENJO and K. IKEUCHI, *Trans. JWRI* **13** (1984) 63.
4. T. ENJO, K. IKEUCHI, M. ANDO and K. HAMADA, *ibid.* **14** (1985) 93.
5. T. LATOUCHE, M. CAILLER and S. K. MARYA, in Proceedings of 4th International Conference on Aluminium Weldments (INALCO, 88), Tokyo, Japan (April, 1988) pp. 21–37.
6. *Idem., Soudage et Techniques Connexes* **43** (1989) 44.
7. *Idem.*, in Proceedings, 4èmes Journées du Soudage (JN4), Paris, March 1989 (Société Française de Métallurgie, Paris, 1989) pp. 54–65.

Received 6 July 1990
and accepted 15 January 1991